ARTICLE

Ultrafast Charge- and Energy-Transfer Dynamics in Conjugated Polymer: Cadmium Selenide Nanocrystal Blends

Frederik S. F. Morgenstern, Akshay Rao, Marcus L. Böhm, René J. P. Kist, Yana Vaynzof, and Neil C. Greenham*

Cavendish Laboratory, University of Cambridge, J. J. Thomson Avenue, Cambridge CB3 0HE, United Kingdom

ABSTRACT Hybrid nanocrystal—polymer systems are promising candidates for photovoltaic applications, but the processes controlling charge generation are poorly understood. Here, we disentangle the energy- and charge-transfer processes occurring in a model system based on blends of cadmium selenide nanocrystals (CdSe-NC) with poly[2-methoxy-5-(3′,7′-dimethyloctyloxy)-1,4-phenylene vinylene] (MDMO-PPV) using a combination of time-resolved absorption and luminescence measurements. The use of different capping ligands (*n*-butylamine, oleic acid) as well as thermal annealing allows tuning of the polymer—nanocrystal interaction. We demonstrate that energy transfer from MDMO-PPV to CdSe-NCs is the dominant exciton quenching mechanism in nonannealed blends and occurs on ultrafast time scales (<1 ps). Upon thermal annealing electron transfer becomes competitive with energy transfer, with a transfer rate of 800 fs independent of the choice of the ligand. Interestingly, we find hole transfer to be much less efficient than electron transfer and to extend over several nanoseconds. Our results emphasize the importance of tuning the organic—nanocrystal interaction to achieve efficient charge separation and highlight the unfavorable hole-transfer dynamics in these blends.

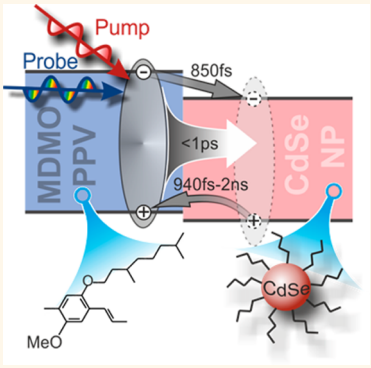

KEYWORDS: nanocrystals · transient absorption · CdSe · polymer · charge transfer · photovoltaics · hybrid · photoluminescence

The prospect of combining the advantageous properties of polymers and nanocrystals in hybrid photovoltaic systems has led to a considerable increase in research interest over the past decade.[1,2] The ability to tune the bandgap in nanocrystals through size control combined with the wide range of organic materials available allows tuning of both optical and electronic properties. Furthermore, semiconducting polymer—nanocrystal blends are generally solution processable and possess the mechanical flexibility inherent to polymers. Concurrently, it is hoped that the high dielectric constants of nanocrystals will aid charge separation and hinder back recombination at the interface.[3] These properties make nanocrystals a promising candidate to replace fullerenes, which are not as widely tunable as nanocrystals, as electron acceptors in organic photovoltaic cells.

Recent studies employing a low-bandgap polymer with CdSe nanodots and tetrapods demonstrated efficiencies of up to 2.7% and 3.1%, respectively.[4,5] While these devices show encouraging performance, solar cells employing nanocrystals as electron acceptors remain outperformed by conventional cells employing fullerene derivatives. Although the electrical characteristics on these polymer—nanocrystal blends have been thoroughly studied, little is known of the underlying charge generation and transfer dynamics that govern device performance. Recently, Colbert *et al.* demonstrated for PbS: poly(2,3-bis(2-(hexyldecyl)quinoxaline-5,8-diyl-*alt*-*N*-(2-hexyldecyl)dithieno[3,2-*b*:2′,3′-d]-pyrrole) blends that charge generation by hole transfer from nanocrystal to polymer is less efficient than by electron transfer from polymer to nanocrystal.[6] However, measuring the actual electron- and hole-transfer rates in these hybrid blends has been challenging.

In the first report of photovoltaics based on cadmium selenide nanocrystals (CdSe-NC) blended with polyphenylenevinylene (PPV) three possible charge-transfer routes were identified[7] (Figure 1a). When the polymer is photoexcited, charges can be generated either (I) directly by electron transfer to the

* Address correspondence to ncg11@cam.ac.uk.

Received for review November 19, 2013 and accepted January 23, 2014.

Published online January 23, 2014
10.1021/nn405978f

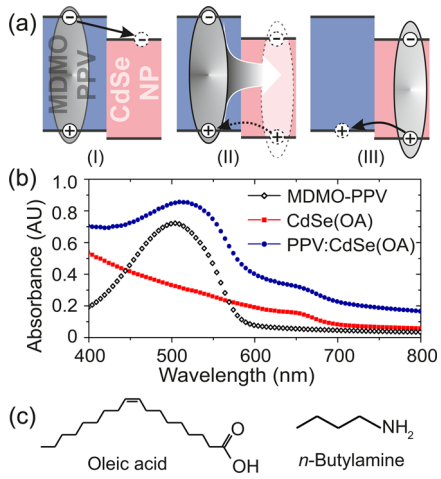

Figure 1. (a) Charge-transfer routes in MDMO-PPV:CdSe-NC blends. Upon photoexcitation of the MDMO-PPV charge separation can occur through (I) electron transfer or *via* (II) Förster resonant energy transfer (FRET) followed by hole-back-transfer. When the exciton is generated in the CdSe-NC, charges can be separated by hole transfer (III) from nanocrystal to polymer. (b) Absorbance spectra of MDMO-PPV, CdSe(OA) nanocrystals, and MDMO-PPV:CdSe(OA) blend. (c) Chemical structures of the ligands used to passivate the CdSe-NCs.

nanocrystal or (II) *via* Förster resonant energy-transfer (FRET) transfer to the nanocrystal followed by hole back-transfer to the polymer. Upon photoexcitation of the nanocrystal, charge generation can occur by (III) hole transfer to the polymer. Time-resolved absorption studies have been employed successfully in the past to investigate charge-transfer rates in donor–acceptor systems such as blends of poly(3-hexylthiophene-2,5-diyl) (P3HT) and [6,6]-phenyl-C61-butyric acid methyl ester (PCBM).[8,9] Polymer–fullerene systems are ideal candidates for transient absorption measurements due to the low optical cross-section of excited states in PCBM combined with the possibility of separately exciting the polymer. In contrast, nanocrystals are relatively strong absorbers in the visible. Although the absorption onset of the nanocrystals can be tuned, employing larger crystals has been found to be crucial for device performance. Thus, for most nanocrystal–polymer systems, such as the CdSe:polyphenylene-vinylene (PPV) system described above, the absorptions of the polymer and nanocrystal overlap. Therefore, upon excitation of the polymer, processes I, II, and III will occur simultaneously, which makes a direct measurement of the various transfer rates difficult. Broad nonlinear contributions to the transient absorption signal arising from biexcitons,[10] charges,[11] and surface traps[12] present an additional obstacle in disentangling these transfer processes. However, a detailed understanding of the underlying transfer rates and potential bottlenecks is crucial for designing improved systems. In this paper, we employ a combination of transient absorption and time-resolved photoluminescence spectroscopy together with a genetic algorithm to study electron-, hole-, and energy-transfer dynamics in the model nanocrystal–polymer system CdSe:polyphenylenevinylene (PPV).[13,14]

RESULTS AND DISCUSSION

Colloidal CdSe-NCs were used as the electron-accepting material and poly[2-methoxy-5-(3′,7′-dimethyloctyloxy)-1,4-phenylene vinylene] (MDMO-PPV) as the hole-transporting donor material. Recent characterization of this system using 3D electron tomography[15] allows us to correlate the photophysics to the nanomorphology of the system. CdSe nanocrystals of 6.1 nm diameter were synthesized using oleic acid (OA) as the capping agent. The nanocrystal size was tuned such that the absorption of the lowest allowed transition ($1S_{3/2}$-$1S_e$)[16] does not overlap significantly with the absorption of the polymer. Absorption spectra for oleic acid capped CdSe nanocrystals (CdSe(OA)), pristine MDMO-PPV, and their blend are shown in Figure 1b.

n-Butylamine-capped CdSe-NCs (CdSe(BUT)) were prepared in a postsynthetic ligand exchange. The chemical structure of the various ligands can be found in Figure 1c. Nanocrystal films and MDMO-PPV blends were spin-coated from chlorobenzene solution on infrared-grade fused silica glass. For MDMO-PPV:CdSe films a 1:9 polymer–nanocrystal mass ratio was used. Further details about synthesis and sample fabrication can be found in the Supporting Information (SI).

By employing different ligands,[17] we were able to modify both the surface passivation and the polymer–nanocrystal spacing without changing the photoactive materials. Oleic acid is the longer ligand, which presumably gives rise to a larger polymer–CdSe distance, while *n*-butylamine can be expected to provide a smaller spacing. In addition, blend films were annealed for 10 min at 140 °C. It is generally accepted that prolonged annealing of nanocrystal films results in the removal of a fraction, but not all, of the capping ligands,[18] with the degree of removal strongly dependent on the ligand type. X-ray photoemission spectroscopy (XPS) measurements conducted on annealed and nonannealed films of CdSe(BUT) and CdSe(OA) are shown in the SI. To verify the nanocrystal quality, MDMO-PPV:CdSe devices were prepared using the same polymer:nanocrystal ratio and annealing procedure. External quantum efficiencies of these devices are shown in the SI.

We begin by using transient absorption (TA) measurements to study the evolution of the system following excitation of the CdSe-NCs with a pump wavelength of 640 nm and a pulse irradiance of 1000 μJ/cm^2. Transient spectra of annealed CdSe(BUT) and MDMO-PPV:CdSe(BUT) are shown in Figure 2. For nanocrystal-only films, we observe a broad and flat positive TA that decays slowly, giving rise to a negative TA signal at times larger than 200 ps. The same broad positive feature is observed in the blend.

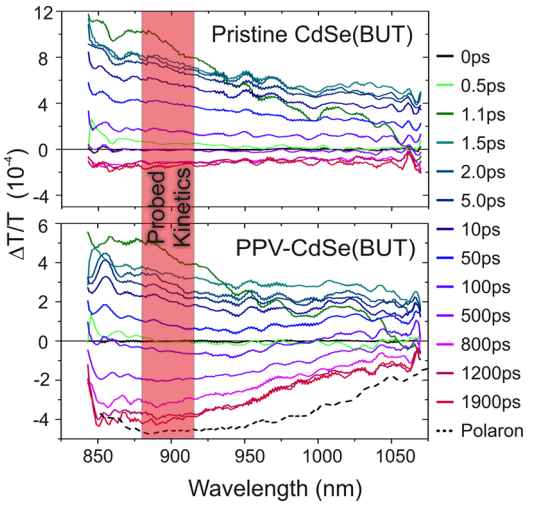

Figure 2. Transient absorption spectra of an annealed CdSe-NC film (top) and a MDMO-PPV:CdSe-NC blend, both using *n*-butylamine as a capping agent. The samples were excited at 650 nm at a pulse irradiance of 1000 μJ/cm^2. The dotted line corresponds to the polaronic signal of a MDMO-PPV:CdSe(BUT) blend upon direct excitation of the PPV (excitation wavelength 520 nm, probed after 2 ns).

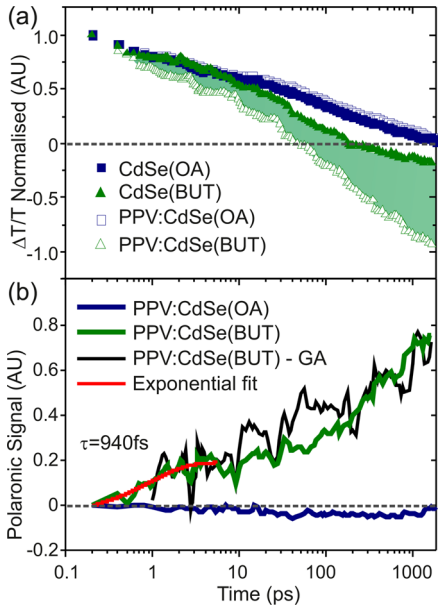

Figure 3. (a) Normalized transient absorption kinetics of annealed MDMO-PPV:CdSe blend (open symbols) and CdSe-NC films (filled symbols) for various ligands, excited at 650 nm and probed between 880 and 920 nm at a pulse irradiance of 1000 μJ/cm^2. The shaded regions indicate the difference in dynamics between blends and nanocrystal-only films. (b) MDMO-PPV hole-polaron signal, obtained by subtracting the blend and nanocrystal-only signals in (a). The black line shows the normalized kinetics of the hole polaron obtained by genetic algorithm simulation (GA). The polaronic kinetics from 200 fs−5.5 ps were fitted using a monoexponential (red curve).

However, unlike the featureless negative TA contribution observed in nanocrystal-only films, blends exhibit a negative TA peak between 850 and 900 nm at times larger than 100 ps. Positive TA features of CdSe nanocrystals in this spectral range are typically attributed to photoluminescence from trap states[19] (see the SI). The negative contribution in nanocrystal-only films in the near-IR is generally associated with the photoinduced absorption (PIA) of charges.[20] It has been proposed that surface traps induce a perturbation to the intraband selection rules, therefore allowing transitions from the quantized excitonic states into the continuum at high energy, resulting in a broad PIA feature in the near IR.[21] In pure CdSe(BUT) films, the PIA manifests itself as a broad flat negative feature at times larger than 500 ps. In PPV:CdSe(BUT) blends an additional species must be present with a transition in the near-IR to account for the PIA peak observed around 880 nm. Hole polarons on MDMO-PPV are known to have an absorption peak between 880 and 920 nm.[22,23] We thus attribute the additional PIA feature in MDMO-PPV:CdSe(BUT) blends to the formation of MDMO-PPV hole-polarons, generated *via* hole transfer from the nanocrystal to the polymer.

Figure 3a shows the kinetics at the absorption peak of the hole polaron, measured between 880 and 920 nm, again exciting the nanocrystal component. The TA signal of the MDMO-PPV:CdSe(BUT) blend is found to decay faster than in its nanocrystal-only counterpart, suggesting interaction with the MDMO-PPV, in line with the change in the TA spectra seen in Figure 2 between *n*-butylamine-capped nanocrystal-only and blend films. In contrast, comparing the TA kinetics of CdSe(OA) and MDMO-PPV:CdSe(OA) films we find that both decay at the same rate within the first two nanoseconds. This suggests that hole transfer from OA-capped CdSe-NC is poor and does not occur within the first 1800 ps.

Figure 3b shows an estimation of the hole polaron signal, which we obtain by taking the difference between the TA signals for nanocrystal-only and blend samples. For MDMO-PPV:CdSe(OA) no polaron signal is observed within the time range of the measurement. In contrast, blends using the much shorter *n*-butylamine ligands show an additional PIA, which rises at 0.3 ps and continues increasing within the experimentally accessible time window of 1800 ps. The initial rise (0.2−5.5 ps) of the polaron signal was fitted using a single-exponential decay function of the form

$$y = A(1 - e_0^{-(t - t_0)/\tau})$$

A time constant of τ = (940 ± 220) fs was obtained. However, only a small fraction of the hole polarons are created within the first 2 ps. The fact that the polaron signal is still rising beyond 1 ns and is observed here at very high excitation fluences suggests that the hole transfer is inefficient even for short *n*-butylamine ligands. We also note that even the fitted initial hole transfer rate is 20 times slower than that observed in MDMO-PPV:PCBM blends.[24] We find the results to be in good agreement with the kinetic traces modeled using

a genetic algorithm (GA) method, described in detail elsewhere.[25] Here, we decompose the TA signal of the polymer−nanocrystal blend in two components. We fix one of them using the TA spectrum of the nanocrystal-only film at 1 ps as a reference. The algorithm then produces a second "charge" spectrum by breeding randomly generated spectra and selecting the ones that in combination with the reference give the best fit to the original data. The "charge" spectrum is constrained such that only spectra with negative sign are considered. The normalized kinetics of the hole polaron obtained *via* this method are found to be in good agreement with the kinetics obtained by the simple subtraction method described above.

The dependence of the hole-transfer rate on the capping ligand indicates that hole transfer is a short-range process and is strongly hindered by long ligands such as oleic acid. While we cannot rule out the possibility that changing the ligand directly influences the hole-transfer rate due to changes in the degree of passivation of nanocrystal surface traps, we note that both the MDMO-PPV:CdSe(OA) and MDMO-PPV:CdSe-(BUT) samples are annealed and are expected to have relatively poor ligand coverage. Hole transfer in both samples is therefore likely to be influenced by unpassivated surface traps to a similar degree. Hence, we consider that differences in spacing between the nanocrystals and polymer are the most likely explanation for the difference in hole-transfer rates in the two samples.

The relatively inefficient hole transfer in samples where a substantial fraction of the nanocrystal surface is likely to be free of ligands is rather surprising. Possible reasons include the need for excitons to migrate between nanocrystals in order to find an interface where charge transfer can occur, the small offset between the HOMO level of the MDMO-PPV (about −5.3 eV)[26] and the valence band of the CdSe-NC (−5.4 eV),[27] or the trapping of holes on the surface of the nanocrystals, leading to states from which it is more difficult for the hole to transfer to the polymer.

To study charge- and energy-transfer dynamics upon excitation of the polymer we used a combination of TA and time-resolved photoluminescence measurements. Figure 4a shows the 2D TA map of MDMO-PPV:CdSe(BUT) probed in the near IR (820−1020 nm) and excited at 530 nm at a pulse irradiance of 8.6 μJ/cm^2. Although the excitation wavelength is close to the absorption peak of the MDMO-PPV, both MDMO-PPV and CdSe-NCs can be excited at this wavelength. The TA signal will therefore contain contributions from excitations generated on the polymer and on the CdSe. Crucially, the optical cross-section of transitions associated with trapped charges and excited species in CdSe-NCs was found to be about 2 orders of magnitude lower than the cross-section of excited species in MDMO-PPV. Considering that the CdSe-NCs absorb about 1.8 times more light at 520 nm than at 640 nm,

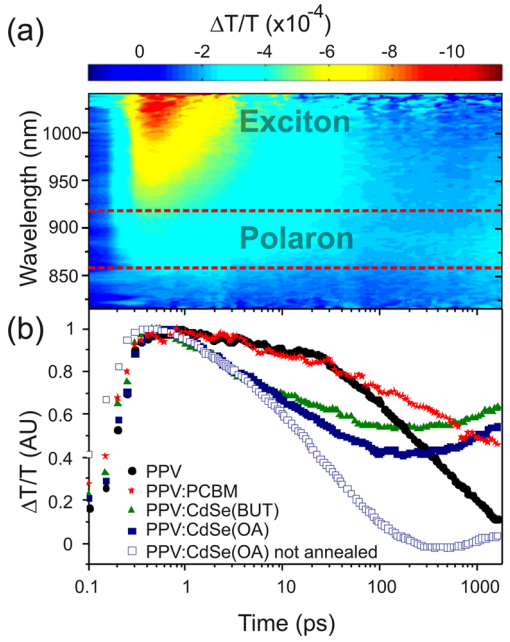

Figure 4. (a) Time-resolved transient absorption spectra of MDMO-PPV:CdSe(BUT) excited at 530 nm at a pulse irradiance of 8.6 μJ/cm^2. The spectral region where the polaron absorbs is marked. (b) Normalized transient absorption kinetics of MDMO-PPV:CdSe-NC blends with different ligands and annealing conditions, probed between 860 and 920 nm. Similar kinetics for a pure MDMO-PPV film and for an MDMO-PPV:PCBM blend are shown for comparison.

CdSe-NCs are expected to have a contribution to the TA signal of about $\Delta T/T = 3 \times 10^{-6}$, which is 2 orders of magnitude lower than signals observed here. Thus, we can neglect contributions from trap absorption and excited species in the CdSe-NC and assume that the TA signal in this spectral region arises solely from excited states on the polymer.

TA kinetics shown in Figure 4b were measured between 860 and 920 nm, at the absorption peak of the hole polaron, and are compared with the kinetics of a pure MDMO-PPV film. The 2D TA map of pure MDMO-PPV is shown in the SI. In the absence of electron acceptors, excitons generated in the pure MDMO-PPV film decay without forming polarons. We thus attribute the negative TA signal in the pure MDMO-PPV film (see the SI) to the PIA from the exciton. When compared to pure MDMO-PPV, all annealed and nonannealed blends showed accelerated decay kinetics (Figure 4b). This suggests that MDMO-PPV excitons are efficiently quenched by the CdSe nanocrystals, independent of the choice of the ligand.

The TA signal for nonannealed MDMO-PPV:CdSe-(OA) blends was found to decay fully within 200 ps. There is no evidence for the formation of long-lived charges in these blends, so we attribute the quenching of the polymer excitons solely to energy transfer from polymer to nanocrystals. It appears that the ligand shell remaining in these nonannealed blends is sufficient to prevent the short-range process of charge transfer,

but the longer range process of energy transfer is still allowed. In contrast, in the two annealed blends the TA signal did not decay fully but reached a plateau within 1 ns. We attribute this long-lived contribution in TA signal to the PIA of the PPV hole polaron. These MDMO-PPV hole polarons can either be generated by direct transfer of the electron or by FRET from the excited MDMO-PPV to an adjacent CdSe-NC, followed by hole back-transfer. However, a number of pieces of evidence suggest that hole back-transfer does not play an important role in charge generation here: (i) charge generation occurs with similar dynamics even in MDMO-PPV:CdSe(OA) blends which as shown above do not undergo hole transfer following nanocrystal excitation; (ii) with nanocrystal excitation, to observe polaron absorptions of similar magnitude to those seen when exciting at 530 nm required 60 times higher excitation densities than those used here, suggesting that the yield of holes from nanocrystal excitons is small; and (iii) the charge generation observed here is complete significantly sooner than the time scales observed earlier for hole transfer. From the measured absorbance of these films (Figure 1) we can estimate the wavelength-dependent charge generation efficiency. Neglecting scattering losses, we find that PPV:CdSe(OA) blends absorb about 85% of the incident light at 530 nm and 50% at 640 nm. If the charge generation were wavelength independent we would expect to generate about twice as many hole polarons when exciting at 530 nm instead of 640 nm. However, since the signal is about 60 times stronger when exciting at 530 nm we conclude that charge generation is not wavelength-independent. Charge separation by hole transfer to the polymer is surprisingly inefficient and does not contribute significantly to charge generation in these films. This is of particular interest when considering that devices fabricated with both oleic acid- and butylamine-capped nanocrystals show a significant contribution to the external quantum efficiency (shown in the SI) in the spectral region where PPV does not (λ > 600 nm) or only weakly absorbs (λ < 400 nm). There are two possible explanations for this trend. Either a significant amount of hole transfer from MDMO-PPV to CdSe occurs only after several nanoseconds, or alternatively, the contribution of the CdSe nanocrystals to photocurrent in the absence of significant hole transfer from the CdSe-NC to MDMO-PPV could suggest that excitons can dissociate in the CdSe nanocrystal network without the need for hole transfer to the polymer. That is, the CdSe is functioning as a "solar cell within a solar cell". Strein *et al.* have shown PbS nanocrystal-polymer blends to be able to operate as quantum dot Schottky diodes, where the polymer acts as an energy-transfer sensitizer to the nanocrystals (assuming the nanocrystals form a percolating pathway).[28] Further studies are required to determine which of these explanations is the most adequate.

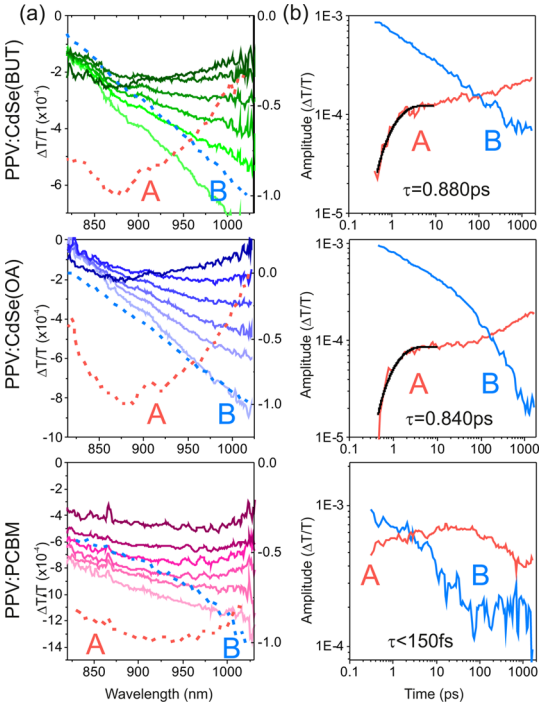

Figure 5. (a) Transient absorption spectra of annealed MDMO-PPV:CdSe(BUT) (top), MDMO-PPV:CdSe(OA) (middle), and MDMO-PPV:PCBM (bottom) excited at 8.6uJ/cm^2. Time slices were taken at 1, 10, 50, 100, and 1700 ps (light to dark colors). "A" and "B" refer to the two spectral components of the TA signal, i.e., the hole polaron (A) and exciton (B) on the MDMO-PPV. For convenience, amplitudes of A and B were normalized to 1 and plotted in the same figure using the right axis. (b) Time evolution of the amplitude of component "A" (polaron) and "B" (exciton). The black curves show mono-exponential fits between 350 fs and 10 ps for the MDMO-PPV:CdSe blends.

Figure 5a shows the TA spectra for PPV:CdSe(BUT), PPV:CdSe(OA), and PPV:PCBM blends in the near-IR region (800−1050 nm) at different times. As seen in Figure 4b all blends show more rapid decay kinetics at the earliest time points, indicating exciton quenching *via* subpicosecond energy and/or charge transfer. To determine the charge-transfer rate more accurately the TA spectra shown in Figure 5a were decomposed into two components using a genetic algorithm (GA) (see the Methods). The two spectra obtained, labeled "A" and "B", are shown by the dashed lines for each blend. Based on previous spectroscopic investigations[23] and using the TA spectrum of pristine MDMO-PPV (SI), we assign spectrum "A" to the PPV hole polaron and "B" to the PPV singlet exciton.

The respective kinetic traces of the hole-polaron signal "A" and exciton signal "B" are shown in Figure 5b. Singlet and hole kinetics in PPV:CdSe blends showed similar trends independent of the capping ligands. While the singlet excitons are fully formed at the earliest times, the hole polarons grow in as the singlets decay. We attribute the initial rise of the hole-polaron signal to electron transfer from MDMO-PPV to the CdSe nanocrystals. The rise of the polaron signal (A)

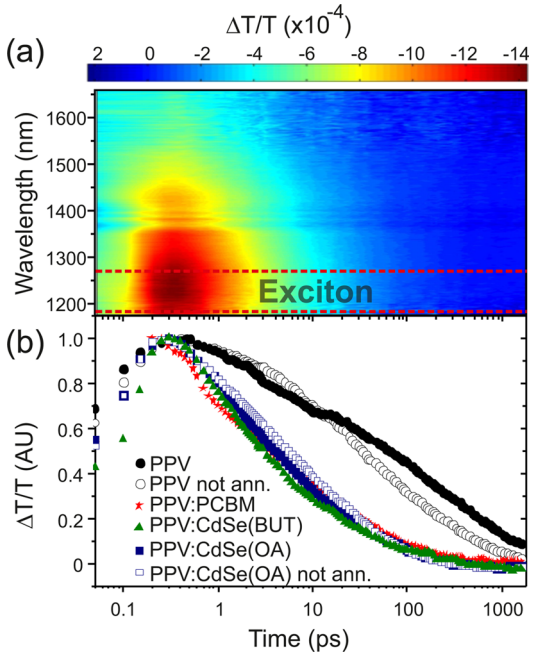

Figure 6. (a) Time-resolved TA spectrum of MDMO-PPV:CdSe(BUT) excited at 530 nm at a pulse irradiance of 8.6 μJ/cm^2 and probed in the near IR (1175−1660 nm). (b) Normalized TA kinetics of the MDMO-PPV singlet exciton measured between 1175 and 1275 nm for MDMO-PPV:CdSe and MDMO-PPV:PCBM blends and for pure MDMO-PPV.

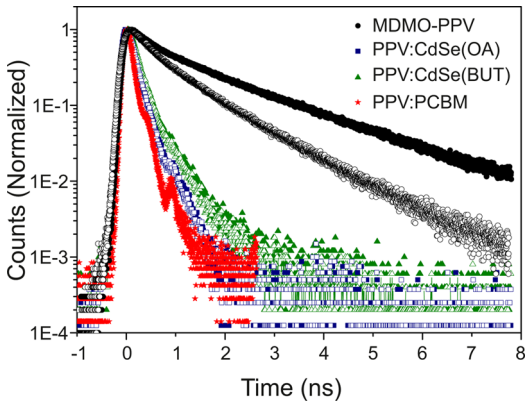

Figure 7. Photoluminescence decay dynamics of pure MDMO-PPV (black circles), MDMO-PPV:CdSe(OA) (blue squares), MDMO-PPV:CdSe(BUT) (green triangles), and MDMO-PPV:PCBM (red stars) excited at 470 nm and probed at 590 nm using time-correlated single-photon counting. Annealed samples are depicted using filled symbols and nonannealed samples using open symbols.

was fitted using a single exponential. Decay constants of τ_{BUT} = (880 ± 200) fs and τ_{OA} = (840 ± 200) fs were found for annealed PPV:CdSe(BUT) and PPV:CdSe(OA) blends. Interestingly, MDMO-PPV:CdSe(OA) blends using the long oleic acid as capping agent showed the same transfer rate as MDMO-PPV:CdSe(BUT). This charge transfer rate is well below the electron transfer rate of PPV:PCBM blends, which occurs below our instrument response (150 fs) and has been reported to occur within 45 fs[22] (Figure 5, bottom). The later rise in hole signal in nanocrystals:polymer blends is likely due to excitons generated in the polymer bulk. These excitons need to diffuse to the interface before they can be dissociated and therefore contribute to the hole TA signal only after several tens of picoseconds.

Further time-resolved TA spectra were measured between 1150 and 1600 nm at a pulse irradiance of 8.6 μJ cm^{-2}. A 2-D map of TA signal over time and wavelength of MDMO-PPV:CdSe(BUT) is shown in Figure 6a. Since PPV polarons have a negligible absorption in this spectral region,[29] we attribute the measured TA signal to the decay of the PPV singlet exciton. Figure 6b shows the TA kinetics of pure MDMO-PPV, MDMO-PPV:CdSe(OA), MDMO-PPV:CdSe(BUT), and MDMO-PPV:PCBM at the PIA peak of the singlet exciton, measured between 1150 and 1250 nm. A strong exciton quenching was observed in all blends, with PPV:PCBM blends showing the fastest initial quenching of the PPV exciton. Although charge transfer occurs on a subpicosecond time scale it takes 20−30 ps for an 80% decay of the excitonic signal. This is true for both annealed nanocrystal−polymer blends where charge transfer is observed as well as the nonannealed blends where excitons are predominantly quenched by energy transfer. The similar excitonic decay in annealed and nonannealed PPV-CdSe(OA) blends further suggests diffusion-limited quenching (see Figure 6b). Only excitons at the polymer−nanocrystal interface are efficiently quenched, and since energy and charge transfer occur on a subpicosecond time scale, exciton kinetics in the picosecond time scale will be dominated by the slow exciton diffusion. This direct measurement of the singlet exciton can furthermore be used to validate the charge transfer kinetics obtained by the GA algorithm. When comparing the extracted singlet exciton kinetics of spectrum "A" to the exciton kinetics measured at 1200 nm, we find the GA singlet kinetics to be in good agreement with the kinetics obtained by direct measurement, suggesting a successful GA decomposition.

To further investigate the exciton diffusion in these blends we studied their luminescence decay when exciting at 470 nm. Figure 7 shows the time-resolved photoluminescence decay of pristine MDMO-PPV as well as of annealed and nonannealed blends of MDMO-PPV:CdSe(BUT), MDMO-PPV:CdSe(OA), and MDMO-PPV:PCBM measured at the peak of the MDMO-PPV emission at 590 nm. Steady-state photoluminescence (PL) spectra for MDMO-PPV and CdSe(BUT) are provided in the SI. The PL from CdSe was found to be very weak, and its contribution was not evident in the blend films. Time-resolved PL of the MDMO-PPV exciton shows a biexponential decay with decay time constants of τ_1 = 374 ps and τ_2 = 1334 ps. The fast decay component is consistent with previous reports of excitonic decay in MDMO-PPV.[30,31] In agreement with the TA measurements shown in Figure 6, all blend films were found to have substantially reduced PL lifetimes. This indicates

that excitons in PPV are efficiently quenched, independent of the choice of the ligand. The respective time constants can be found in the SI. Nonannealed blends decayed with the same rate as their annealed counterparts. Since excitons in nonannealed PPV:CdSe(OA) are quenched by FRET and excitons in annealed PPV:CdSe(OA) are largely quenched by charge transfer, their common decay kinetics suggest that PL kinetics are dominated by a slower process which precedes energy and charge transfer. This is consistent with the exciton-diffusion-limited quenching observed in TA kinetics of Figure 6.

Changes in the photoluminescence decay between MDMO-PPV:CdSe blends using different ligands therefore indicate differences in the average exciton diffusion time and give insight into the morphology of the blend. Blends using oleic acid were found to have the faster exciton quenching than MDMO-PPV:CdSe(BUT), suggesting a finer morphology. Atomic force microscopy images shown in the SI further support this. MDMO-PPV:CdSe(OA) blends revealed a lower surface roughness than their MDMO-PPV:CdSe(BUT) counterparts, consistent with a finer intermixing.

CONCLUSIONS

We have investigated the different possible charge- and energy-transfer routes in MDMO-PPV:CdSe-NC blends and correlated the respective transfer rates to the ligand treatment of the CdSe-NC. In nonannealed blends with long ligands the FRET mechanism was found to dominate exciton quenching, with a subpicosecond transfer rate for excitons at the interface. Electron transfer was found to be independent of the capping ligands, with a transfer rate of ~940 fs. We found the rate of PPV exciton quenching, both from charge transfer and energy transfer to be dominated by the diffusion of the excitons to the interface, as indicated by TA and PL measurements. Hole transfer from CdSe-NC to MDMO-PPV exhibited a much stronger dependence on the capping ligands and therefore on polymer−nanocrystal separation and was only observed for MDMO-PPV:CdSe blends using the short *n*-butylamine ligands. Although there is some subpicosecond hole transfer in MDMO-PPV:CdSe(BUT) blends, only a small fraction of the initial excitation was found to lead to polaron generation. Interestingly, hole transfer from the nanocrystal to the polymer was observed up to several nanoseconds in MDMO-PPV:CdSe(BUT) blends. Considering that a large fraction of the excitons are generated in the CdSe-NC, inefficient hole-transfer from the CdSe-NC to the polymer should result in MDMO-PPV:CdSe cells having a negligible contribution from CdSe-NC to photocurrent. The fact that we observe considerable photocurrent generation even for oleic acid capped CdSe-NCs could suggest that the CdSe nanocrystal network in these cells operates as a "solar cell within a solar cell", with exciton dissociation occurring in the CdSe without the need for a hole-accepting polymer.

METHODS

Nanocrystal Synthesis. All chemicals were purchased from Sigma-Aldrich unless stated otherwise. CdSe-nanocrystals and the corresponding ligand exchange procedures where performed using standard air-free techniques. CdO (0.748 g, 5.8 mmol, 99.99%) was blended with oleic acid (OA, 28.7 mL, 90.6 mmol, analytical standard) and 1-octadecene (ODE, 19 mL, analytical). The solution was degassed under vacuum (<0.1 mbar) at 100 °C for 2 h and subsequently set under inert atmosphere at 230 °C. Separately, two Se-precursor solutions, containing 0.345 g (4.4 mmol, 99.999%, Alfa Aeser) of Se and 4. (10.0 mmol, 97%) of *n*-trioctylphosphine, respectively, were prepared in a nitrogen-filled glovebox. The selenium precursor solutions were consecutively injected with an interval of 15 min into the Cd/OA/ODE solution at 230 °C under inert atmosphere. After a total reaction time of 1 h, the solution was quenched to room temperature by injection of 5 mL of methanol and by placing the reaction flask into a water bath. The crude solution was purified by multiple precipitation cycles with a 2-propanol/methanol mixture and toluene. The final oleic acid capped product was redispersed in octane to yield a final concentration of ca. 100 mg/mL.

Ligand Exchange. For ligand-exchange reactions to *n*-butylamine, 250 mg of CdSe NPs was dispersed in toluene to yield a concentration of 50 mg/mL. After addition of *n*-butylamine (1.6 mL, 16 mmol, >99.5%), the solution was stirred for 12 h at room temperature. The final product was purified by precipitation with a 2-propanol/methanol mixture and redispersion in hexane. To separate further byproducts the solution was centrifugated in hexane. For device processing the supernatant was finally flocculated by the same 2-propanol/methanol mixture and redispersed in chlorobenzene.

Transient Absorption Spectroscopy. For TA spectroscopy, samples were excited with narrowband (20 nm) ultrafast pulses derived from the output of a 1 kHz regenerative amplifier (Spectra-Physics Solstice), which was used to seed a traveling optical parametric amplifier (TOPAS) (Light Conversion). The transmission of the sample was probed using the broadband (850−1050 nm) output of a home-built noncollinear optical parametric amplifier. The probe beam was split to provide a reference signal, which does not interact with the pump, to mitigate the effect of laser fluctuations. The probe and reference signals were dispersed in a spectrometer (Andor, Shamrock SR-303i) and detected using a pair of 16-bit 1024-pixel linear image sensors (Hamamatsu, S8381-1024Q), which were driven and read out at 1 kHz by a custom-built board from Stresing Entwicklunsbuero.

Conflict of Interest: The authors declare no competing financial interest.

Supporting Information Available: X-ray photo electron spectroscopy (XPS), photoluminescence data, and atomic force microscopy (AFM). This material is available free of charge *via* the Internet at http://pubs.acs.org.

Acknowledgment. This work was supported by the Engineering and Physical Sciences Research Council (Grant No. EP/G060738/1). A.R. thanks Corpus Christi College for a Research Fellowship.

REFERENCES AND NOTES

1. Lee, H.; Yum, J.; Leventis, H.; Zakeeruddin, S. M.; Haque, S. A.; Chen, P.; Seok, S. I.; Grätzel, M.; Nazeeruddin, M. K. CdSe Quantum Dot-Sensitized Solar Cells Exceeding Efficiency 1% at Full-Sun Intensity. *J. Phys. Chem. C* **2008**, *112*, 11600–11608.

2. Nozik, A. J.; Beard, M. C.; Luther, J. M.; Law, M.; Ellingson, R. J.; Johnson, J. C. Semiconductor Quantum Dots and Quantum Dot Arrays and Applications of Multiple Exciton Generation to Third-Generation Photovoltaic Solar Cells. *Chem. Rev.* **2010**, *110*, 6873–6890.
3. Li, Z.; Gao, F.; Greenham, N. C.; McNeill, C. R. Comparison of the Operation of Polymer/Fullerene, Polymer/Polymer, and Polymer/Nanocrystal Solar Cells: A Transient Photocurrent and Photovoltage Study. *Adv. Funct. Mater.* **2011**, *21*, 1419–1431.
4. Zhou, Y.; Eck, M.; Veit, C.; Zimmermann, B.; Rauscher, F.; Niyamakom, P.; Yilmaz, S.; Dumsch, I.; Allard, S.; Scherf, U. Efficiency Enhancement for Bulk-Heterojunction Hybrid Solar Cells Based on Acid Treated CdSe Quantum Dots and Low Bandgap Polymer PCPDTBT. *Sol. Energy Mater. Sol. Cells* **2011**, *95*, 1232–1237.
5. Dayal, S.; Kopidakis, N.; Olson, D. C.; Ginley, D. S.; Rumbles, G. Photovoltaic Devices with a Low Band Gap Polymer and CdSe Nanostructures Exceeding 3% Efficiency. *Nano Lett.* **2010**, *10*, 239–242.
6. Colbert, A. E.; Janke, E. M.; Hsieh, S. T.; Subramaniyan, S.; Schlenker, C. W.; Jenekhe, S. A.; Ginger, D. S. Hole Transfer from Low Band Gap Quantum Dots to Conjugated Polymers in Organic/Inorganic Hybrid Photovoltaics. *J. Phys. Chem. Lett.* **2013**, *4*, 280–284.
7. Greenham, N. C.; Peng, X.; Alivisatos, A. P. Charge Separation and Transport in Conjugated-Polymer/semiconductor-Nanocrystal Composites Studied by Photoluminescence Quenching and Photoconductivity. *Phys. Rev. B* **1996**, *54*, 17628–17637.
8. Piris, J.; Dykstra, T. E.; Bakulin, A. A.; Van Loosdrecht, P. H. M.; Knulst, W.; Trinh, M. T.; Schins, J. M.; Siebbeles, L. D. A. Photogeneration and Ultrafast Dynamics of Excitons and Charges in P3HT/PCBM Blends. *J. Phys. Chem. C* **2009**, *113*, 14500–14506.
9. Marsh, R. A.; Hodgkiss, J. M.; Friend, R. H. Direct Measurement of Electric Field-Assisted Charge Separation in Polymer:fullerene Photovoltaic Diodes. *Adv. Mater.* **2010**, *22*, 3672–3676.
10. Kambhampati, P. Unraveling the Structure and Dynamics of Excitons in Semiconductor Quantum Dots. *Acc. Chem. Res.* **2011**, *44*, 1–13.
11. Burda, C.; Link, S.; Mohamed, M.; El-Sayed, M. The Relaxation Pathways of CdSe Nanoparticles Monitored with Femtosecond Time-Resolution from the Visible to the IR: Assignment of the Transient Features by Carrier Quenching. *J. Phys. Chem. B* **2001**, *105*, 12286–12292.
12. Saari, J. I.; Dias, E. a; Reifsnyder, D.; Krause, M. M.; Walsh, B. R.; Murray, C. B.; Kambhampati, P. Ultrafast Electron Trapping at the Surface of Semiconductor Nanocrystals: Excitonic and Biexcitonic Processes. *J. Phys. Chem. B* **2013**, *117*, 4412–4421.
13. Ginger, D.; Greenham, N. Charge Separation in Conjugated-Polymer/Nanocrystal Blends. *Synth. Met.* **1999**, *101*, 425–428.
14. Ginger, D.; Greenham, N. Photoinduced Electron Transfer from Conjugated Polymers to CdSe Nanocrystals. *Phys. Rev. B* **1999**, *59*, 10622–10629.
15. Hindson, J. C.; Saghi, Z.; Hernandez-Garrido, J.-C.; Midgley, P. A.; Greenham, N. C. Morphological Study of Nanoparticle-Polymer Solar Cells Using High-Angle Annular Dark-Field Electron Tomography. *Nano Lett.* **2011**, *11*, 904–909.
16. Efros, A. L.; Rosen, M. The Electronic Structure of Semiconductor Nanocrystals. *Annu. Rev. Mater. Sci.* **2000**, *30*, 475–521.
17. Olson, J. D.; Gray, G. P.; Carter, S. A. Optimizing Hybrid Photovoltaics through Annealing and Ligand Choice. *Sol. Energy Mater. Sol. Cells* **2009**, *93*, 519–523.
18. Niu, Y. H.; Munro, A. M.; Cheng, Y.-J.; Tian, Y. Q.; Liu, M. S.; Zhao, J. L.; Bardecker, J. A.; Jen-La Plante, I.; Ginger, D. S.; Jen, A. K.-Y. Improved Performance from Multilayer Quantum Dot Light-Emitting Diodes via Thermal Annealing of the Quantum Dot Layer. *Adv. Mater.* **2007**, *19*, 3371–3376.
19. Underwood, D. F.; Kippeny, T.; Rosenthal, S. J. Ultrafast Carrier Dynamics in CdSe Nanocrystals Determined by Femtosecond Fluorescence Upconversion Spectroscopy. *J. Phys. Chem. B* **2001**, *105*, 436–443.
20. McArthur, E. A.; Morris-Cohen, A. J.; Knowles, K. E.; Weiss, E. A. Charge Carrier Resolved Relaxation of the First Excitonic State in CdSe Quantum Dots Probed with Near-Infrared Transient Absorption Spectroscopy. *J. Phys. Chem. B* **2010**, *114*, 14514–14520.
21. Tyagi, P.; Kambhampati, P. False Multiple Exciton Recombination and Multiple Exciton Generation Signals in Semiconductor Quantum Dots Arise from Surface Charge Trapping. *J. Chem. Phys.* **2011**, *134*, 094706.
22. Montanari, I.; Nogueira, A. F.; Nelson, J.; Durrant, J. R.; Winder, C.; Loi, M. A.; Sariciftci, N. S.; Brabec, C. Transient Optical Studies of Charge Recombination Dynamics in a Polymer/fullerene Composite at Room Temperature. *Appl. Phys. Lett.* **2002**, *81*, 3001.
23. Scharber, M.; Winder, C.; Neugebauer, H.; Sariciftci, N. Anomalous Photoinduced Absorption of Conjugated Polymer/fullerene Mixtures at Low Temperatures and High Frequencies. *Synth. Met.* **2004**, *141*, 109–112.
24. Bakulin, A. A.; Hummelen, J. C.; Pshenichnikov, M. S.; van Loosdrecht, P. H. M. Ultrafast Hole-Transfer Dynamics in Polymer/PCBM Bulk Heterojunctions. *Adv. Funct. Mater.* **2010**, *20*, 1653–1660.
25. Gélinas, S.; Paré-Labrosse, O. The Binding Energy of Charge-Transfer Excitons Localized at Polymeric Semiconductor Heterojunctions. *J. Phys. Chem. C* **2011**, *115*, 7114–7119.
26. Mühlbacher, D.; Neugebauer, H.; Cravino, A.; Sariciftci, N. S. Comparison of Electrochemical and Spectroscopic Data of the Low-Bandgap Polymer PTPTB. *Mol. Cryst. Liq. Cryst.* **2002**, *385*, 205–213.
27. Jasieniak, J.; Califano, M.; Watkins, S. E. Size-Dependent Valence and Conduction Band-Edge Energies of Semiconductor Nanocrystals. *ACS Nano* **2011**, *5*, 5888–5902.
28. Strein, E.; Colbert, A.; Subramaniyan, S.; Nagaoka, H.; Schlenker, C. W.; Janke, E.; Jenekhe, S. a.; Ginger, D. S. Charge Generation and Energy Transfer in Hybrid Polymer/infrared Quantum Dot Solar Cells. *Energy Environ. Sci* **2013**, *6*, 769.
29. Brabec, C. J.; Zerza, G.; Cerullo, G.; De Silvestri, S.; Luzzati, S.; Hummelen, J. C.; Sariciftci, S. Tracing Photoinduced Electron Transfer Process in Conjugated Polymer/Fullerene Bulk Heterojunctions in Real Time. *Chem. Phys. Lett.* **2001**, *340*, 232–236.
30. Van Hal, P. A.; Wienk, M. M.; Kroon, J. M.; Verhees, W. J. H.; Slooff, L. H.; van Gennip, W. J. H.; Jonkheijm, P.; Janssen, R. A. J. Photoinduced Electron Transfer and Photovoltaic Response of a MDMO-PPV:TiO_2 Bulk-Heterojunction. *Adv. Mater.* **2003**, *15*, 118–121.
31. Offermans, T.; van Hal, P.; Meskers, S.; Koetse, M.; Janssen, R. Exciplex Dynamics in a Blend of π-Conjugated Polymers with Electron Donating and Accepting Properties: MDMO-PPV and PCNEPV. *Phys. Rev. B* **2005**, *72*, 1–11.